

# Preliminary Design Review: Exploring the Feasibility of Human Life on Venus

Justin Bak - jb2757

Due Date: May 6th, 2025

# Contents

<b>Introduction</b>	<b>3</b>
Objectives and Success Criteria . . . . .	3
Storyboard . . . . .	4
VISTA Mission Event Timeline . . . . .	4
<b>Subsystems</b>	<b>6</b>
Subsystems Overview . . . . .	6
Key Subsystems . . . . .	6
Other Subsystems . . . . .	11
Total Size Weight and Power (SWaP) Estimation . . . . .	12
Trade Studies . . . . .	12
<b>Risk Assessment</b>	<b>20</b>
Technical Risks . . . . .	20
Cost Risks . . . . .	21
Risk Matrix . . . . .	21
<b>CDR Plan</b>	<b>23</b>
Long Lead Items . . . . .	23
<b>Appendices</b>	<b>26</b>
Appendix A . . . . .	26
Appendix B . . . . .	28
Appendix C . . . . .	31

## Introduction

For decades, the idea of human life in the Venusian atmosphere has been conceptualized. The Venusian In Situ Tropospheric Aerostat (VISTA) is a robotic balloon-based platform designed to assess the feasibility to human life in the upper atmosphere of Venus. To perform this study, VISTA aims to collect high-fidelity data on thermal conditions, atmospheric chemistry, radiation levels, and wind dynamics through a robotic payload over the course of 30 Earth days. In this report, the viability of the VISTA mission is evaluated through an initial timeline of the mission, overview of the subsystems, trade studies, and a risk assessment.

## Objectives and Success Criteria

The primary objective of the VISTA mission is to assess the feasibility of human life in the upper atmosphere of Venus (altitude of 50 - 60 km). This region has pressure and temperature conditions surprisingly similar to those found on Earth's surface, with temperatures ranging from 20 degrees to 70 degrees Celsius and a pressure of approximately 1 atm. However, the environment is far more hostile from the pervasive clouds of sulfuric acid and high levels of solar and infrared radiation, making Venus' troposphere a challenging location for long-duration exploration. Due to these conditions, a crewed mission to Venus is infeasible given current technology. VISTA proposes a fully robotic approach to studying the environmental conditions of the region of interest, suspended at constant altitude via aerostat. VISTA then aims to capture and transmit environmental data to Earth, which can be used to develop technology capable of one day sending humans to the Venusian atmosphere.

The success criteria of VISTA is organized to properly determine the safety of future human missions to the upper atmosphere of Venus. The primary success criterion is that the aerostat shall deploy and inflate within the range of 50-60 km in altitude. This criterion is addressed first as VISTA cannot properly collect and transmit environmental data typical of Earth surface conditions outside of this altitude range. Furthermore, VISTA is at risk of being lost in the intense gravitational pull of Venus below this altitude range, and could be subject to harsher winds. Additionally, VISTA shall acquire and transmit high-resolution atmospheric pressure, temperature, chemical composition, and wind profile data. This criterion is put at risk by component failure or communications blackout. The final success criterion centralizes around operational longevity: VISTA shall operate continuously for at least 30 Earth days while maintaining attitude control and power balance. This criterion is mainly at risk from sulfuric acid corrosion and harsh winds in the Venusian atmosphere (240 km/h). Extended mission success is also contingent on operational lifetime, which is achieved at operational lifetime twice that of full mission success (60 days).

## Storyboard

The storyboard of the VISTA mission is visualized below with a corresponding timeline that describes each event.



Figure 1: Storyboard of VISTA [7] [8]

### VISTA Mission Event Timeline

- **Venus Transfer & Arrival**

After a 6-month cruise from Earth, VISTA arrives at Venus and begins orbit insertion using onboard propulsion and precise attitude control. A final burn completes the Hohmann transfer. This marks the beginning of entry operations.

*Timeline: Unknown*

- **Aerobraking & Entry**

VISTA uses controlled atmospheric drag to slow down and transition from interplanetary orbit into an entry trajectory toward the upper atmosphere. Entry conditions are carefully monitored to ensure thermal and structural loads remain within limits. Aerobraking reduces the velocity to a point suitable for aerostat deployment.

*Timeline: Within hours of arrival*

- **Envelope Deployment & Inflation**

At an altitude of approximately 50 km, VISTA ejects its aeroshell and autonomously inflates its helium-based aerostat. Successful inflation is critical for achieving neutral buoyancy and mission survival. A failed inflation results in mission termination shortly after entry.

*(Partial Mission Success)*

*Timeline: 30–60 minutes after entry*

- **System Check**

VISTA conducts a full systems health check, verifying thermal control, pressure integrity, sensor function, and communication systems. Any anomalies are flagged for corrective action. This ensures the platform is safe for continued operation and science collection.

*Timeline: 15–30 min after inflation*

- **Instrument Activation**

Onboard scientific instruments and payloads power on and calibrate to begin atmospheric and environmental data acquisition. Sensor diagnostics confirm calibration accuracy and functional readiness. Calibration data are transmitted to Earth for confirmation.

*Timeline: 10–15 min after system check*

- **Atmospheric Composition Survey**

VISTA continuously records atmospheric pressure, temperature, wind speed, and gas composition. These data help assess environmental habitability and support models of Venusian atmospheric structure. The survey remains active for the duration of the mission.

*(Full Mission Success)*

*Timeline: Begins 1 hr post-deployment; ongoing*

- **Acidic Cloud Sampling**

Specific surfaces are exposed to Venus' sulfuric acid-rich atmosphere and monitored for corrosion effects. Data collected will inform material selection for future missions involving long-term Venusian exposure. Initial observations begin shortly after deployment.

*Timeline: Begins 2–3 hrs after deployment; ongoing*

- **Radiation & Solar Monitoring**

VISTA measures incident solar flux and ambient radiation levels to characterize energy availability and radiation shielding needs. These measurements support thermal and power system design for future atmospheric missions.

*Timeline: Begins alongside Event 6; continuous*

- **Altitude Modulation**

VISTA adjusts its altitude by venting gas or adjusting internal pressure to study different atmospheric layers. Altitude control enables targeted sampling and helps characterize vertical structure and buoyancy dynamics.

*Timeline: Begins Day 2; occurs regularly*

- **Wind & Turbulence Mapping**

Wind speed, direction, and shear are recorded to characterize atmospheric stability and dynamic loading. Turbulence data contribute to improved modeling of the Venusian climate and inform future aerostat control strategies.

*Timeline: Begins Day 1–2; evaluated continuously*

- **Data Transmission**

Scientific data and system health updates are transmitted back to Earth via direct or relay communication. Downlink efficiency is monitored and adjusted based on bandwidth availability and communication geometry.

*Timeline: Begins Day 1; occurs regularly*

- **Extended Mission / Descent**

If conditions remain favorable, VISTA will either continue long-duration monitoring beyond 30 days or descend into denser layers for high-risk science goals. This phase represents an opportunity to stretch mission capabilities beyond primary objectives.

*(Extended Mission)*

*Timeline: Begins Day 30+ (if successful)*

It is important to note that the timeline for event one is unknown as there is a trade-off to be discussed on the travel of VISTA from low Earth orbit (LEO) to low Venusian orbit (LVO). This trade-off is regarding the use of chemical propulsion or electric propulsion and is largely time dependent.

## **Subsystems**

This section presents the functional baseline for the VISTA system, organized by subsystem, emphasizing the space segment, the ground segment, key performance metrics, and the rationale behind selected subsystem architectures through relevant trade studies.

### **Subsystem Overview**

The VISTA spacecraft is organized into the following subsystems:

1. **Payload**
2. **Communications**
3. **Power Generation and Storage**
4. **Buoyancy and Altitude Control**
5. **Command & Data Handling (C&DH)**
6. **Thermal Control**
7. **Attitude Determination & Control (ACS)**
8. **Structure and Materials**

Each subsystem performs essential functions to support the scientific and operational goals of the mission. Each subsystem will be briefly discussed, but for the sake of this report, only four of these—Payload, Communications, Power, and Buoyancy/Altitude Control—will be discussed in detail due to their central role in enabling habitability assessment and maintaining system viability in Venus' harsh environment.

### **Key Subsystems**

#### **Payload**

The payload is the foremost important subsystem as it determines the rest of the mission architecture. In the case of VISTA, the payload consists of environmental sensors, imaging devices, and chemical analysis tools designed to characterize the upper atmosphere of Venus. These instruments include UV/IR spectrometers, pressure/temperature sensors, gas chromatograph, and high-resolution cameras. It is in the best interest of the mission to use commercial-off-the-shelf (COTS) components for the payload to leverage proven performance and cut on development costs. However, the 96% sulfuric acid aerosol environment at 50 km altitude requires that any COTS component be coated or enclosed in corrosion-resistant housings.

To achieve the desired mission goal, three components are necessary: a spectrometer, pressure/temperature sensors, and a camera system. On the discussion of spectrometers, Ocean Insight's Flame-T and Hamamatsu's mini-spectrometers (e.g., C12880MA) offer UV/VIS/NIR coverage in compact, space-adaptable formats. These sensors are most pertinent to the chemical composition of Venus and the underlying metals which could possibly collide with the aerostat, causing mission failure. To gauge pressure and temperature, rugged balloon-borne sensors can be adapted to withstand the harsh Venusian atmosphere. Paroscientific's MET4 is found to be a cost efficient solution, but it is not rated for the increased temperature at this altitude of Venus' atmosphere [6]. One solution is to utilize this sensor in conjunction with TEConnectivity's FLIR A700, which is rated for a higher temperature. In terms of camera systems, space-hardened versions of Teledyne e2v CMOS sensors and FLIR's Quark thermal imaging cores offer modular imaging solutions [4]. Using a COTS approach, it is easier to determine a preliminary power, weight, and size estimation (PWaS) as a summation of all the values from the specification sheets:

<b>Component (COTS Product)</b>	<b>Mass (kg)</b>	<b>Power (W)</b>	<b>Volume (m<sup>3</sup>)</b>
Ocean Insight Flame-T Spectrometer (2x)	0.27	3.6	0.0004
Hamamatsu C12880MA Mini Spectrometer (Backup)	0.005	0.1	0.000025
TE Connectivity MS8607 P/T Sensors (4x)	0.004	0.2	0.00001
Custom MEMS Gas Chromatograph (est.)	1.2	8.0	0.001
FLIR Quark 2 Thermal Imaging Core	0.05	2.0	0.0001
<b>Total (COTS Payload)</b>	<b>1.53</b>	<b>13.9</b>	<b>0.0015</b>

Table 1: COTS-Based Payload PWaS Estimate (Converted to m<sup>3</sup>)

## Communications

According to the System Requirements Review, the VISTA mission will need a high bandwidth, low-latency communication system to transmit atmospheric data. This is to be accomplished via direct transmission to Earth or through an orbiter relay satellite. As Venus is 38 million kilometers away from Earth at its closest approach, the direct-to-Earth transmission approach yields higher delay times (5 - 15 minutes). Optical communications were considered to mitigate this lag, but this requires precise pointing, which is infeasible in the Venusian atmosphere, where sulfuric clouds block laser communication and winds rage up to 240 km/hr [14]. While a dedicated relay satellite is ideal for continuous communication, there is currently no operational Venus orbiter equipped to serve as a communication relay for interspacecraft links. JAXA's Akatsuki remains active but is not configured for relay operations [9]. NASA's upcoming Venus missions, VERITAS and DAVINCI, are scheduled for launch no earlier than 2031. These orbiters may become potential relay assets depending on their architecture and inter-satellite compatibility, but they are not guaranteed resources for a VISTA mission launched in the near term [3] [11].

Additionally, the VISTA system operates in the X-band, which is commonly used for planetary communications due to its lower susceptibility to atmospheric attenuation and its balance between antenna size and bandwidth. Ka-band offers significantly higher data rates and spectral efficiency, but is more prone to signal degradation from Venus' thick clouds and requires more precise pointing and more complex hardware. Given these tradeoffs, X-band is preferred for reliability and power efficiency in this mission context.

The power estimates for the communications subsystem are based on benchmarks from NASA's Iris X-band transponder and small satellite communication FPGAs, which draw between 25 and 35 W during burst transmission. Processing power (7 W) accounts for data compression, routing, and transmission scheduling onboard [5].

To validate feasibility of communication over interplanetary distances, the power flux density at Earth from VISTA can be modeled using the inverse square law:

$$P_{\text{flux}} = \frac{P_T}{4\pi R^2}$$

Assuming a transmitter power  $P_T = 28 \text{ W}$  and Venus-Earth closest approach distance of  $R = 3.8 \times 10^{10} \text{ m}$ , we get:

$$P_{\text{flux}} \approx \frac{28}{4\pi(3.8 \times 10^{10})^2} \approx 1.55 \times 10^{-22} \text{ W/m}^2$$

This received power level is extremely low, but remains within the detectable range of the Deep Space Network (DSN) when using a high-gain directional antenna, justifying VISTA's communication architecture.

The volume of the communications subsystem is based on the envelope required to house the X-band transceiver, processing electronics, and a steerable high-gain antenna system. Based on dimensions from small satellite platforms (e.g., Iris or Innocomm X-band radios), we estimate a volume of approximately  $0.012 \text{ m}^3$ . This accommodates heat shielding, RF isolation, and cable routing. This also correlates to a mass of about  $10 \text{ kg}$ .

## Power

The power subsystem comprises of deployable solar panels and high-density battery storage. As VISTA's operational lifetime may exceed the nominal mission duration, it is essential to provide a regenerative power source. Venus offers an unusually high solar flux (approximately 1.9 times greater than that at Earth) making solar power a particularly attractive solution for sustained operations in its upper atmosphere. The solar panels on the aerostat are therefore the main power source, optimized for diffused light through the dense cloud layer of Venus. Batteries provide power continuity during night-side operations or periods of obscuration.

The power system's total average output and component sizing were determined based on subsystem-level power draws and the expected operational profile. The following equations were used to estimate the required solar array area and battery storage:

### 1. Total Power Budget (with margin):

$$P_{\text{total}} = \sum P_i + M_p \quad (\text{where margin } M_p = 30\%)$$

Assuming  $P_i \approx 180 \text{ W}$ , we obtain:

$$P_{\text{total}} = 180 \times 1.3 = 234 \text{ W}$$

### 2. Solar Array Area:

$$A_{\text{array}} = \frac{P_{\text{total}}}{\eta \cdot S_{\text{Venus}}}$$

Where:

- $\eta = 0.28$  (solar array efficiency)
- $S_{\text{Venus}} \approx 2611 \text{ W/m}^2$

$$A_{\text{array}} = \frac{234}{0.28 \cdot 2611} \approx 0.32 \text{ m}^2$$



### 3. Battery Storage for Eclipse or Obscured Periods:

$$E_{\text{battery}} = \frac{P_{\text{avg}} \cdot t_{\text{dark}}}{\eta_{\text{battery}}}$$

With  $P_{\text{avg}} = 180 \text{ W}$ ,  $t_{\text{dark}} = 1 \text{ hour}$ , and  $\eta_{\text{battery}} = 0.9$ , we get:

$$E_{\text{battery}} = \frac{180 \cdot 1}{0.9} \approx 200 \text{ Wh}$$

This confirms that the selected battery capacity of approximately 800 Wh is more than sufficient to handle multiple cycles of low-light operation, with redundancy and buffer.

### Buoyancy and Altitude Control

Once the aerostat has been deployed, it is important to remain at 50 km in altitude for data return as the cloud deck at 50 km contains sulfuric acid aerosols and dynamic chemistry that influence the planet's radiation balance and atmospheric structure. Studying this layer allows VISTA to directly measure variables like UV absorption, sulfur chemistry, trace gas content, and vertical wind shear, which are all relevant to evaluating the habitability and stability of a floating platform.

To accomplish this, VISTA aims for passive buoyancy control while enabling controlled modulation of altitude for science operations. Lift is generated through a large, helium-filled balloon envelope constructed from acid-resistant film. This will ensure the passive state of VISTA in the atmosphere, whereas the active control will be achieved through gas venting and ballast ejection. The venting is used to decrease volume and reduce buoyancy if descent is required. This process can be managed by automated vent valves connected to internal pressure sensors. To ascend or regain altitude lost due to atmospheric variability, the system can release a small amount of stored solid or liquid ballast, reducing mass and increasing net lift. This capability allows VISTA to perform vertical profiling of the atmosphere over time.

To calculate the volume of helium required to support the system at 50 km altitude in Venus' atmosphere, we use Archimedes' principle, where we imply the total system mass as 200 kg [1]:

$$\Delta M = V \cdot (\rho_{\text{atm}} - \rho_{\text{He}})$$

Where:

- $\Delta M$ : net lift mass (kg), equal to system mass
- $V$ : volume of the balloon ( $\text{m}^3$ )
- $\rho_{\text{atm}} = 1.2 \text{ kg/m}^3$ : density of Venus' atmosphere at 50 km
- $\rho_{\text{He}} = 0.18 \text{ kg/m}^3$ : density of helium at the same altitude

Solving for  $V$ :

$$V = \frac{M_{\text{sys}}}{\rho_{\text{atm}} - \rho_{\text{He}}} = \frac{200}{1.2 - 0.18} \approx 196.1 \text{ m}^3$$

Assuming a spherical balloon, the radius  $r$  is calculated using the volume formula:

$$V = \frac{4}{3}\pi r^3 \Rightarrow r = \left(\frac{3V}{4\pi}\right)^{1/3}$$

$$r = \left( \frac{3 \cdot 196.1}{4\pi} \right)^{1/3} \approx 3.60 \text{ m} \Rightarrow \text{Diameter} = 2r \approx 7.20 \text{ m}$$

This balloon sizing provides sufficient lift to counteract a 200 kg payload, with margin for ballast, thermal expansion, and operational altitude variability. As the buoyancy system is mostly passive, there is no power requirement other than a brief pulse for altitude gain/loss around 1-2 W.

In the original concept proposed in the SRR, two blimp structures are suspending the payload. However, due to stability issues, VISTA now opts for a single balloon approach. To develop the profile of the balloon, we use an optimization technique 'fmincon' in MATLAB. Beginning with a volume of 200 m<sup>3</sup>, we aim to optimize the volume of the balloon, requiring the crown radius to be 3.60 m. The code then separates the profile into 'n' gores, which in the provided case is 12. This will enhance manufacturing efficiency of the balloon. This code can be found in Appendix A. The balloon profile and gore profile can be found below:

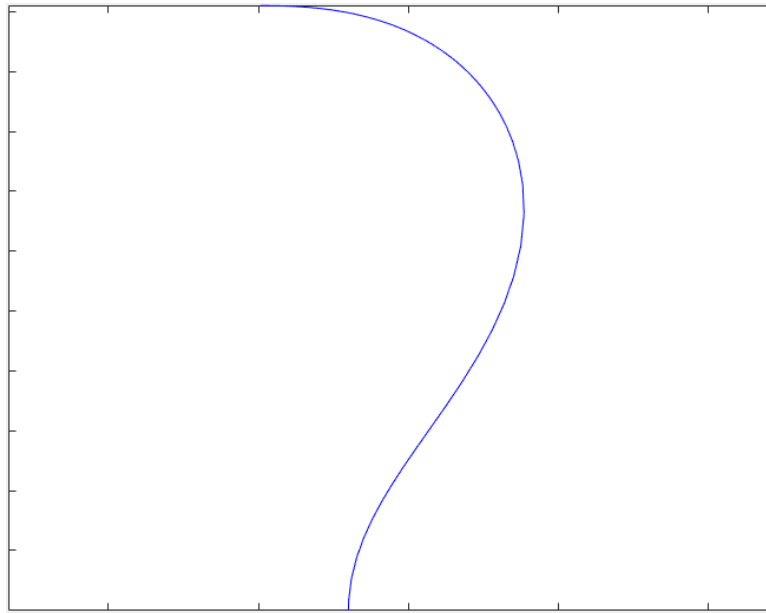


Figure 2: Balloon Profile of VISTA

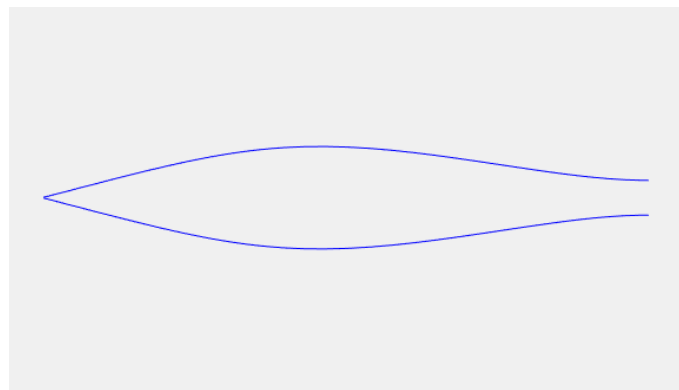


Figure 3: Gore Profile of VISTA

## **Other Subsystems**

### **Command & Data Handling (C&DH)**

The C&DH subsystem serves as the central processing unit of VISTA, coordinating command execution, subsystem interfacing, data routing, and autonomous operations. It collects telemetry and science data from all onboard systems, applies data compression and prioritization routines, and schedules packets for transmission via the communications subsystem. The C&DH system continuously monitors spacecraft health, runs a real-time fault detection and recovery (FDIR) routine, and can reconfigure key functions in response to anomalies. It operates with a low-power processor or FPGA, interfacing with redundant non-volatile memory for data buffering. The architecture supports autonomous operations for up to 30 days without Earth intervention, ensuring mission continuity even during communication blackouts.

### **Thermal Control**

The thermal control subsystem ensures that all onboard systems remain within operational temperature limits despite Venus' challenging thermal environment. At 50 km altitude, ambient temperatures range from approximately 70°C to 120°C. VISTA uses a combination of multilayer insulation (MLI), acid-resistant thermal blankets, and passive radiators to manage heat exchange. Internally, heat pipes conduct excess heat away from sensitive electronics to external radiators. Most thermal regulation is passive to conserve power, but the system includes a limited number of active thermal switches or thermostatically controlled heaters to protect batteries and compute elements during night-side operation or transient cooling events. The gondola structure is thermally isolated from the balloon envelope to reduce external heat conduction, and thermal coatings are used to reflect a portion of the intense solar flux at Venus' proximity to the Sun.

### **Attitude Determination & Control (ACS)**

The attitude control system for VISTA must perform maneuvering both in Venusian orbit and control of the aerostat once it has been deployed. If possible, it would be ideal to use similar components for the in-orbit and on-planet attitude control systems. For in-orbit attitude control, typical technologies include reaction wheel arrays (RWAs), control moment gyros (CMGs), and cold-gas thrusters. A further discussion on the Attitude Control System can be found below in the trade studies.

### **Structure and Materials**

As pictured in the SRR, VISTA's structural system is designed to provide mechanical support, environmental protection, and modular integration of all subsystems while minimizing mass. The gondola frame is constructed from lightweight titanium alloy, selected for its excellent strength-to-weight ratio and inherent resistance to high temperatures and sulfuric acid corrosion. External panels are coated in PTFE (Teflon) to provide chemical shielding against the dense acidic aerosol layer at 50 km altitude. All seams and cable interfaces are sealed using gaskets and boots to prevent acid ingress. The balloon envelope is fabricated from fluorinated ethylene propylene (FEP) or ETFE, which offer the flexibility needed for deployment and inflation, along with sufficient tensile strength and resistance to UV degradation. The structural design must accommodate launch loads, thermal expansion, and vibration, as well as maintain gondola integrity during descent and inflation events. Internal mounting racks are thermally isolated and vibration-damped to protect COTS electronics and instruments.

## Total Size Weight and Power (SWaP) Estimation

From all the previous subsystems, we can tabulate all sizes, weights, and power intakes to find the total system SWaP estimation:

Subsystem	Volume (m <sup>3</sup> )	Mass (kg)	Power (W)
Payload (COTS + science instruments)	0.0015	18	40
Communications (X-band, steerable)	0.012	10	35
Power System (solar + batteries)	0.025	25	200 (gen.)
Buoyancy/Altitude Control	196.15	15	5
C&DH	0.005	8	20
Thermal Control	0.010	5	5
ADCS (reaction wheels, IMUs)	0.008	6	10
Structure and Materials	0.150	100	0 (passive)
<b>Total (Estimated)</b>	<b>196.3265</b>	<b>187</b>	<b>115 (avg)</b>

Table 2: Estimated Volume, Mass, and Power Consumption by Subsystem

## Trade Studies

### Communications Options

As previously discussed, the atmosphere of Venus makes it exceedingly difficult to utilize any communication technologies which require precise pointing. Given this constraint along with limited onboard power, the communication system must balance performance, reliability, and simplicity. Two architectural options were considered: direct-to-Earth (DTE) communication and a relay satellite configuration.

Direct-to-Earth (DTE) communication allows VISTA to transmit signals directly to Earth-based receivers, such as NASA's Deep Space Network (DSN). While this approach simplifies mission architecture and avoids the need for a secondary spacecraft, it has several drawbacks. The balloon platform lacks the pointing precision of an orbiting satellite or stabilized spacecraft, making it difficult to align a narrow high-gain antenna with Earth. A relay satellite architecture addresses many of these challenges, in which VISTA transmits data to an orbiting spacecraft, which then relays the information to Earth. This enables lower-power burst transmissions from VISTA and offloads the high-gain, Earth-pointing communications to the relay. It also increases the frequency of communication windows and reduces the pointing requirements. However, no such relay currently exists at Venus. NASA's VERITAS and DAVINCI missions, both scheduled to launch no earlier than 2031, may offer future opportunities if they are equipped for inter-spacecraft communication. For a near-term VISTA mission, this would require launching a dedicated relay satellite as part of the mission architecture.

Ultimately, a relay satellite is chosen as the preliminary design choice for VISTA for its higher efficiency and reliability. As CONOps for VISTA is taking place in 2025, it is likely that it would not launch before NASA's VERITAS and DIVINCI missions, so relay communication options will be available.

### Attitude Control

VISTA's ACS must operate across two fundamentally different mission environments: space and atmosphere. During the interplanetary cruise and Venus arrival, precise attitude control is needed to align solar arrays, correct trajectory, and orient the aeroshell for atmospheric entry. During the balloon phase,

attitude control becomes a matter of gondola stabilization, sensor pointing, and solar tracking. With these dual-phase requirements, several candidate architectures were evaluated.

The first option is a reaction wheel and IMU system, commonly used in small spacecraft. Reaction wheels offer low-power, precise 3-axis control and are ideal for cruise operations and fine stabilization once deployed. However, they saturate easily and may struggle to maintain control during the dynamic entry phase. Their performance is ideal during long, stable operations but limited during high-torque events. The second option is a reaction control system using cold gas thrusters. Thrusters provide the most forceful attitude corrections, which is advantageous during orbital insertion and especially reentry, where the aeroshell must maintain a heat-shield-forward orientation. While this makes RCS attractive for critical entry moments, it is not sustainable for long-duration atmospheric operation due to propellant constraints, especially on a mass-limited balloon platform. A third option, control moment gyroscopes (CMGs), was considered but ruled out due to their mechanical complexity, high power draw, and torque levels being unnecessary for a platform of VISTA's mass and stability requirements.

The proposed design solution for VISTA is a hybrid system: a thruster-based system for coarse attitude maneuvers and reentry orientation during the orbital phase, and a reaction wheel + IMU package for low-power pointing and gondola stabilization in the atmospheric phase. This approach ensures high control authority when it matters most and energy-efficient, passive stability once deployed in Venus' upper atmosphere.

## **Structure and Materials**

VISTA's structural and material choices are driven by three primary environmental challenges: (1) long-duration exposure to sulfuric acid aerosols at 50 km altitude, (2) ambient temperatures ranging from 70–120°C, and (3) the need for a lightweight but mechanically robust frame that supports the gondola, instrumentation, and balloon interface.

For the gondola frame, three material options are considered: aluminum alloys, titanium alloys, and carbon fiber composites. Aluminum is lightweight and cost-effective but is highly vulnerable to corrosion in acidic environments and loses strength at elevated temperatures. Carbon fiber offers exceptional strength-to-weight performance but is sensitive to both chemical degradation and temperature cycling. Titanium alloys (e.g., Ti-6Al-4V) offer the best compromise: they are naturally corrosion-resistant, retain strength at high temperatures, and have extensive flight heritage in chemically aggressive environments. The trade-off is higher cost and slightly higher density, but the penalty is acceptable within the structural budget of VISTA.

For the external skin and protective housing, VISTA compares PTFE (Teflon), ETFE (Ethylene Tetrafluoroethylene), and PEEK (Polyether ether ketone). PTFE is highly flexible, chemically inert, and exceptionally resistant to sulfuric acid, making it a strong candidate for both the gondola outer layer and exposed sensor covers. ETFE is lighter and easier to thermobond, but less resistant to chemical attack. PEEK offers excellent mechanical properties and thermal stability, but is significantly more expensive and heavier. PTFE was selected due to its excellent acid resistance, flexibility, and long-duration durability, particularly in high-altitude balloon applications.

The balloon envelope material must be lightweight, strong, and gas-retentive while resisting UV degradation and sulfuric acid. A multi-layer fluoropolymer laminate with a base of FEP (Fluorinated Ethylene Propylene) is selected. FEP offers better acid resistance and has a proven record in stratospheric balloon systems.

## Propulsion System

VISTA requires a propulsion system capable of transferring the spacecraft from low Earth orbit (LEO) to Venus. Two primary trajectory architectures were considered: a chemical Hohmann transfer and a low-thrust electric propulsion spiral trajectory. The selected propulsion system directly influences launch vehicle requirements, mission duration, and system complexity.

The first option is a chemical propulsion system, which would perform a traditional Hohmann transfer, which uses a single impulsive maneuver to escape Earth's gravity well and inject the spacecraft on a heliocentric transfer trajectory to Venus. Upon arrival, a second burn (or aerobraking) is used to insert into Venus' atmosphere[2]. This approach is well-understood, offers short transfer times of approximately 120–180 days, and minimizes spacecraft complexity. The downsides are the requirement for a significant amount of chemical propellant and a high-thrust engine, which increases the spacecraft's mass and volume.

To obtain definitive values for the Hohmann transfer of interest, a MATLAB code is developed with specific quantities pertinent to the VISTA mission. This code can be found in Appendix C.

In the context of VISTA, the required  $\Delta v$  to transfer a spacecraft from Low Earth Orbit (LEO) to Low Venus Orbit (LVO) was calculated using a series of Hohmann transfer trajectories. The analysis is divided into three distinct phases, each addressing a specific segment of the journey: escaping Earth's orbit, interplanetary transfer, and capturing into Venusian orbit. An important fact to note is the Hohmann transfer is a simplified approach negligent of mass. While the Hohmann transfer is a good initial approach, the reality of the mission may require additional  $\Delta v$  budgeting. The analysis is based upon the theory below:

## Semi-Major Axis

The semi-major axis ( $a_{\text{transfer}}$ ) is the average of the radii of the initial ( $r_p$ ) and final ( $r_a$ ) orbits.

$$a_{\text{transfer}} = \frac{r_p + r_a}{2}$$

## Orbital Velocity at a Given Radius

The orbital velocity ( $v$ ) at any point in the orbit is calculated using the vis-viva equation:

$$v = \sqrt{\mu \left( \frac{2}{r} - \frac{1}{a} \right)}$$

where  $\mu$  is the gravitational parameter ( $GM$ ), where  $G$  is the gravitational constant:

$$G = 6.67 \times 10^{-11} \text{ Nm}^2/\text{kg}^2$$

and  $M$  is the mass of the central body.

## Initial and Transfer Velocity

$$v_{\text{initial}} = \sqrt{\frac{\mu}{r_p}}$$
$$v_{\text{transfer, periapsis}} = \sqrt{\mu \left( \frac{2}{r_p} - \frac{1}{a} \right)}$$

The first impulsive burn is performed at periapsis, where the change in velocity is defined as:

$$\Delta v_1 = v_{\text{transfer, periapsis}} - v_{\text{initial}}$$

### Final and Transfer Velocity

$$v_{\text{final}} = \sqrt{\frac{\mu}{r_a}}$$

$$v_{\text{transfer, apoapsis}} = \sqrt{\mu \left( \frac{2}{r_a} - \frac{1}{a} \right)}$$

The second impulsive burn is performed at apoapsis, where the change in velocity is defined as:

$$\Delta v_2 = v_{\text{final}} - v_{\text{transfer, apoapsis}}$$

The total  $\Delta v$  is the sum of  $\Delta v_1$  and  $\Delta v_2$ .

### Orbital Period of the Elliptical Transfer Orbit

To determine the transfer time for a Hohmann transfer, the orbital period of the elliptical transfer orbit is calculated using:

$$T = 2\pi \sqrt{\frac{a_{\text{transfer}}^3}{\mu}}$$

Since a Hohmann transfer involves traversing only half of the elliptical orbit, the transfer time is:

$$t_{\text{transfer}} = \frac{T}{2} = \pi \sqrt{\frac{a_{\text{transfer}}^3}{\mu}}$$

After inputting values into the code, the results are as follows:

Table 3: Low-Thrust Maneuver Summary for LEO to LVO Transfer [10]

Maneuver	$\Delta v$ (m/s)
LEO to Earth Escape	3,155.38
Interplanetary Departure	2,498.75
Venus Arrival Braking	2,710.52
Venus SOI to LVO	4,155.61
<b>Total <math>\Delta v</math></b>	<b>6,209.50</b>
<b>Transfer Time : 14,191,986.66 s (164.26 days)</b>	

We consider hydrazine ( $\text{N}_2\text{H}_4$ ) as our propellant due to its relatively higher specific impulse and proven track record in the industry. The accompanying oxidizer is commonly nitrogen tetroxide ( $\text{N}_2\text{O}_4$ ).

From the MATLAB results, we know our  $\Delta v$  for the combined Hohmann transfer maneuver is approximately 6.209 km/s. Using this value along with our specific impulse, we can find the required mass of propellant using the rocket equation:

$$m_0 = m_f e^{\Delta v / u_e}$$

Using this equation, where  $u_e = I_{sp}g_0$ , we obtain an initial mass of 1649.24 kg, meaning if VISTA should opt with a chemical propulsion approach, the mass of propellant would be 1449.24 kg.

The second option considered was a low-thrust electric propulsion system (e.g., ion or Hall-effect thrusters), which slowly spirals out of LEO over several months before reaching an interplanetary trajectory. This method is highly propellant-efficient, requiring far less onboard fuel, and is attractive for mass-limited missions. However, it demands a continuous, high-power electrical supply, increasing the burden on the power system. Additionally, electric propulsion would lengthen the transfer time to 9–12 months or more, delay mission science, and require the spacecraft to operate autonomously for a prolonged period in deep space.

To obtain definitive quantities for use of electric propulsion, we input the 200 kg dry mass quantity from the initial SWaP estimate into a MATLAB script which models three low-thrust burns: first to escape LEO, an interplanetary transfer, then entry into LVO. The script also assumes performance metrics from Hall Effect Thrusters. This script can be found in Appendix B. The results are tabulated below:

Table 4: Low-Thrust Maneuver Summary: Mass, Time, and Energy

Parameter	Value
Initial Mass	200.00 kg
Burn 1 Time	115.74 days
Burn 1 Final Mass	143.60 kg
Burn 2 Time	115.74 days
Burn 2 Final Mass	87.19 kg
Burn 3 Time	115.74 days
Burn 3 Final Mass	30.78 kg
Total Time	0.951 years
Total Propellant Mass ( $m_p$ )	169.22 kg
Total $\Delta v$	1089.65 km/s
Power Required	0.611 kW

Compared to chemical propulsion (1449.24 kg), electric propulsion offers a much smaller propellant mass at only 169.22 kg. However, using three low-thrust maneuvers increases transfer time by a factor of 2.11, from 164.26 days to 0.951 years. Given the payload is entirely robotic, the increase in transfer time is a justified expenditure when considering the significant decrease in propellant mass. Thus, the final propulsion system chosen to mitigate mission cost for VISTA is a succession of three low-thrust maneuvers using Hall Effect thrusters. A visual representation of the orbit path is shown below:



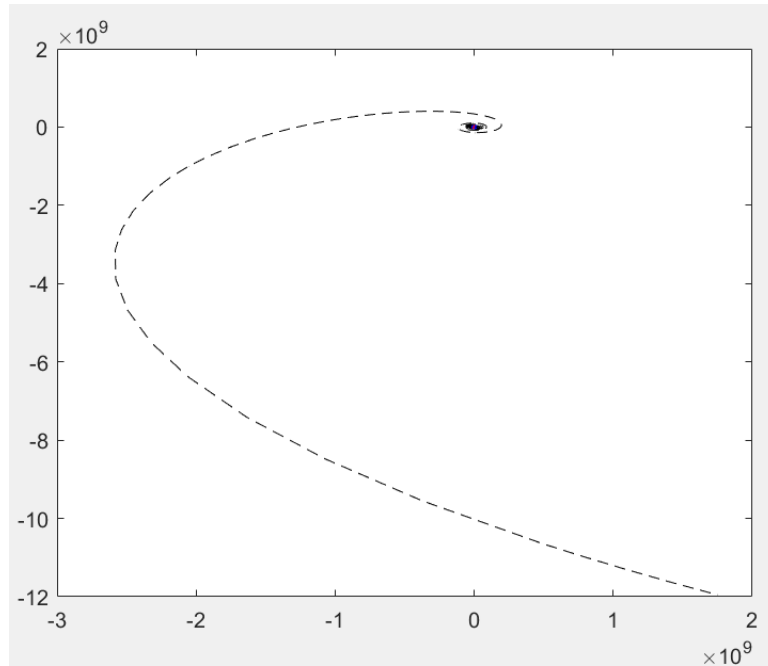


Figure 4: Low Thrust EP Maneuvers Zoomed Out

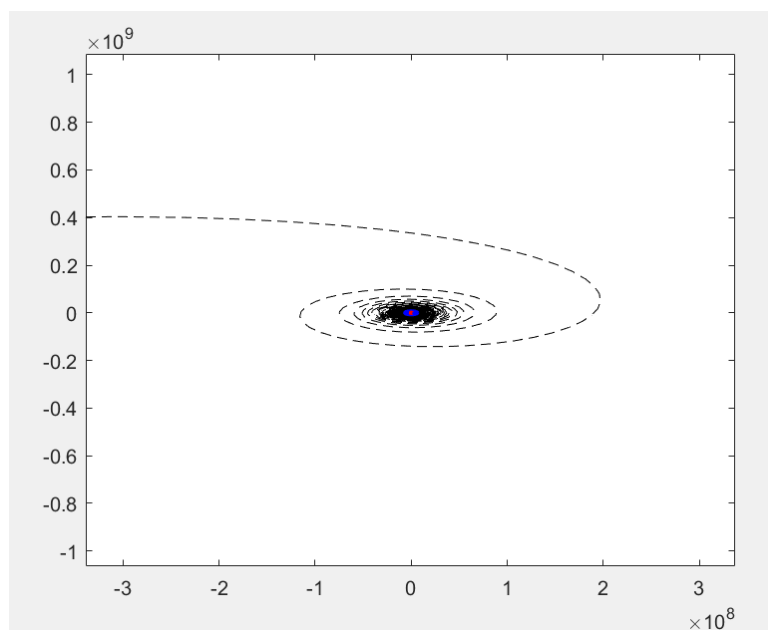


Figure 5: Low Thrust EP Maneuvers Zoomed In

### Launch Vehicle Study

Now that we know the wet mass of the spacecraft (369.22 kg), we can determine an updated SWaP table using the density of our propellant, which we will assume to be Xenon.

Subsystem	Volume (m <sup>3</sup> )	Mass (kg)	Power (W)
Payload (COTS + science instruments)	0.0015	18	40
Communications (X-band, steerable)	0.012	10	35
Power System (solar + batteries)	0.025	25	200 (gen.)
Buoyancy/Altitude Control	1.962 (stowed)	15	5
C&DH	0.005	8	20
Thermal Control	0.010	5	5
ADCS (reaction wheels, IMUs)	0.008	6	10
Propellant Tank (Xenon)	0.197	169.22	0.611
Structure and Materials	0.150	100	0
<b>Total (Estimated)</b>	<b>2.371</b>	<b>356.22</b>	<b>115 (avg)</b>

Table 5: Updated Estimated Volume, Mass, and Power Consumption by Subsystem

Using previous literature, we expect the stowed configuration of the balloon to be about 1% of the deployed volume. Now that the stowed configuration volume and mass of VISTA is known, a trade study on launch vehicle to LEO can be done. Upon reviewing literature on modern launch vehicles, three viable options are found for transport to LEO:

Launch Vehicle	Fairing Volume (m <sup>3</sup> )	LEO Capacity (kg)
Rocket Lab Neutron	30–40	13,000
SpaceX Falcon 9	145	22,800
Firefly Alpha	12.5	1,030
Arianespace Vega C	28	2,300
Rocket Lab Electron	1.2	300
Astra Rocket 3.3	3.0	150
ULA Vulcan Centaur	138	27,200
Relativity Terran R	100	33,500

Table 6: Fairing Volume and LEO Capacity of Candidate Launch Vehicles

Upon reviewing the table, the Rocket Lab Electron and Astra Rocket 3.3 are eliminated from contention as design sacrifices must be made to fit the fairing requirements. These vehicles offer insufficient volume and payload capacity to support the VISTA platform's stowed dimensions and total mass.

The most common option in the current industry landscape is the SpaceX Falcon 9. Its high payload capacity and spacious 5.2-meter diameter fairing offer ample margin for both the mass and volume of the stowed VISTA spacecraft. Additionally, Falcon 9's rideshare program provides a cost-effective launch path, making it accessible for smaller missions like VISTA. However, rideshare flights limit control over orbital parameters and schedule, which could constrain mission timing and transfer optimization. Despite this, Falcon 9 remains a highly reliable and widely used launch vehicle, well-suited to VISTA's requirements.

In Table 6, two candidates arise as the closest match for fairing volume and mass capacity: the Firefly Alpha and Arianespace Vega C. Firefly Alpha is an emerging small launch vehicle designed to deliver up to 1,030 kg to LEO, offering substantial payload margin for the VISTA mission's estimated mass of 356 kg. With a fairing volume of 4.3 m<sup>3</sup>, it accommodates VISTA's 2.37 m<sup>3</sup> stowed volume with ample room for integration hardware and mechanical tolerances. The generous capacity provides flexibility for future payload additions or subsystem growth without requiring redesign. Furthermore, Firefly's relatively low cost per kilogram and focus on dedicated small satellite launches offer schedule reliability and launch flexibility. However, as a newer entrant in the market, Alpha has limited flight heritage compared to more

established launchers, introducing a degree of risk in terms of reliability and availability.

The Vega C is a proven European launch vehicle with extensive flight heritage and strong institutional support from the European Space Agency (ESA). With a payload capacity of approximately 2,200 kg to LEO and a fairing volume of 4.0 m<sup>3</sup>, Vega C comfortably accommodates both the mass and volume of the VISTA spacecraft. Its precision injection capability and integration with ESA's infrastructure ensure robust launch operations and risk mitigation through experience. However, Vega C's launch costs are higher than those of newer commercial alternatives, and European launch scheduling may be more constrained due to institutional payload prioritization. Additionally, while the vehicle has strong heritage, the emphasis on rideshare missions may reduce flexibility for dedicated flight windows unless a custom arrangement is negotiated. Nonetheless, Vega C offers a dependable and technically sound option for VISTA's deployment.

VISTA will utilize the Vega C launch vehicle due to its superior payload capacity, proven reliability, and alignment with European institutional infrastructure. With the ability to deliver up to 2,200 kg to low Earth orbit and a spacious fairing volume of 4.0 m<sup>3</sup>, Vega C fully accommodates the VISTA spacecraft's mass and dimensional requirements. Furthermore, Vega C's precision orbital injection capability and extensive flight heritage provide a strong foundation for mission assurance and risk mitigation. While alternative commercial options like Firefly Alpha offer lower costs, their limited payload capacity, reduced heritage, and higher operational risk make them less suitable for a mission of VISTA's complexity and criticality. Therefore, Vega C presents the most dependable and technically appropriate choice for ensuring the success of the VISTA mission.

# **Risk Assessment**

## **Technical Risks**

### **Balloon Deployment**

Perhaps the most pertinent risk to mission success is the deployment of the aerostat itself. For most satellites with deployable structures, deployment is the most critical part of the mission architecture. However, most of these spacecraft are in orbit, while VISTA must deploy the aerostat as it reenters the atmosphere of Venus. Thus, timing is crucial. If the balloon fails to fully deploy or inflate at the target altitude (50 km), VISTA may descend uncontrollably or be rendered inoperable. This risk stems from the mechanical complexity of deploying a large, folded envelope in an acidic, turbulent environment while ensuring proper inflation sequencing with helium or ammonia gas. Venus' super-rotating winds may further complicate inflation dynamics.

To mitigate this risk, research will be conducted on the best deployment methods for high altitude balloon missions (NASA, JAXA, etc.). Furthermore, an optimization study will be conducted for an ellipsoidal balloon to find desirable geometry characteristics such as throat radius, chord radius, height, etc. If there was not a financial constraint, VISTA's deployable structure could be fabricated and subject to different vibrational and temperature tests.

### **Communications Blackout**

Due to the thick cloud cover of Venus and the long interplanetary communication link, there is a significant risk of communication degradation or loss during mission operations. VISTA relies on burst-mode data transmission using X-band systems to transmit atmospheric and health data either directly to Earth or via a relay satellite. Given that no operational Venus relay currently exists, communications may be limited by geometry, antenna gain, and atmospheric attenuation. Extended communication loss could result in lost data, reduced situational awareness, or an inability to issue corrective commands. These outages could also delay science return or disrupt onboard mission scheduling.

To mitigate this risk, VISTA will implement a backup S-band, low data-rate, low bandwidth system. This way, if the X-band system of communication is lost VISTA can still transmit data back to Earth. Furthermore, VISTA will size the system with buffering capacity to store 7-10 days of data on board. If VISTA experiences blackout, there is a time delay for data so that 'lost' data can be transmitted after blackout. More research will be conducted on communications budget from past Venus missions to establish a blackout tolerance and protocols for if such an event occurs.

### **Long Term Corrosion**

VISTA is intended to operate for a minimum of 30 days in Venus' upper atmosphere, where it will be continuously exposed to sulfuric acid aerosols. While the airship will use acid-resistant materials, there remains a risk that long-term corrosion could degrade structural elements, power conductors, sensor housings, or communication apertures. Corrosion-related failure could compromise data integrity, weaken structural supports, or disable critical systems. The challenge lies not just in selecting acid-resistant materials, but also in ensuring that all exposed seals, joints, and cable interfaces remain intact over time.

Materials such as PTFE, FEP, titanium alloys, and fluoropolymer-coated surfaces will be used in all

externally exposed areas [12]. The design will avoid crevices and unshielded fasteners to reduce acid ingress. Components will be validated via accelerated corrosion testing, including spray chamber exposure, to simulate the mission duration. Additionally, VISTA will include redundant sensors and environmental monitoring to detect early signs of degradation, allowing the system to take preemptive action if necessary.

## Cost Risks

### Launch Integration Delays

As a secondary payload or co-manifested mission, VISTA may rely on shared launch infrastructure with a relay orbiter or future planetary science mission. Any delay or restructuring of the primary launch manifest could cause schedule slippage or force costly design changes to meet new vehicle constraints. This integration dependency introduces uncertainty into the program timeline, with cascading impacts on hardware delivery, testing schedules, and operational planning. In the worst case, if no compatible primary mission emerges, VISTA would require a standalone launch, increasing cost and complexity.

To adhere to these constraints, VISTA will ensure that it fits within reasonable size and mass constraints (e.g., 1.5 m fairing diameter, 200 kg wet mass). This way, VISTA can find other rideshare options if a partnership causes the launch to be delayed in any way.

## Risk Matrix

A risk matrix is included below to better understand both the likelihood and intensity of each technological risk:

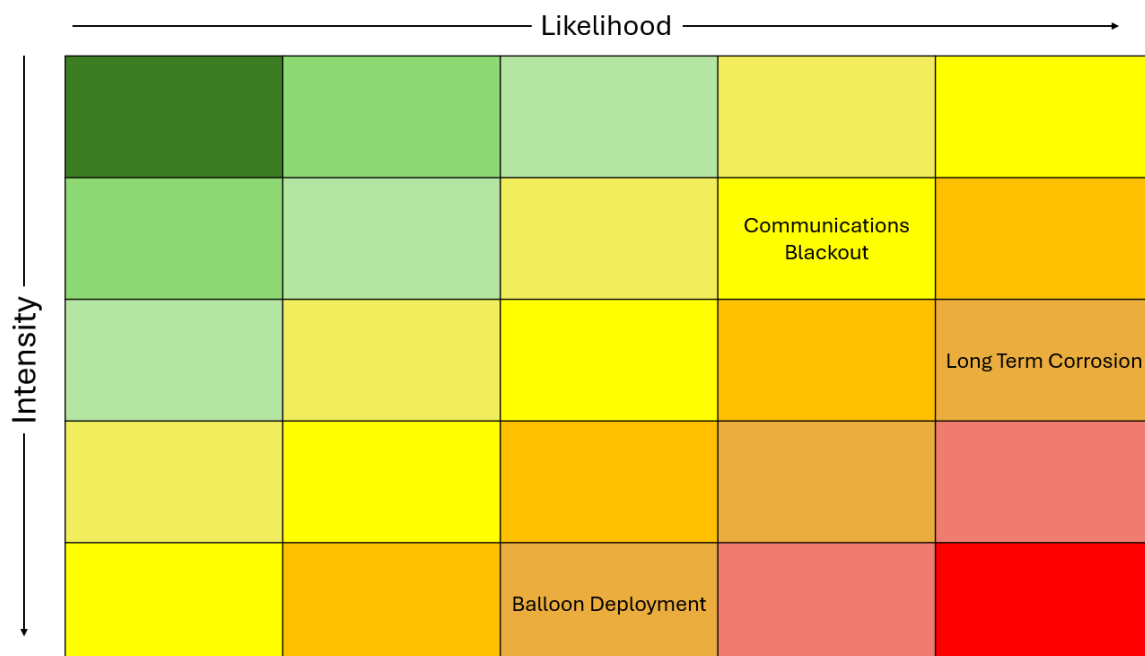


Figure 6: Technological Risk Matrix

Balloon Deployment is assessed a likelihood rating of 3 and an intensity factor of 5. The intensity factor of 5 is given because if the aerostat fails to deploy, the entire mission fails. However, through mitigation

factors, the likelihood of this event occurring has decreased from a rating of 4 to a rating of 3. Due to the success of the VEGA mission, the balloon inflation mechanism is assessed a TRL of 7 as it has displayed success in a mission environment [13]. Communications Blackout is assessed a likelihood rating of 4 and an intensity factor of 2. The likelihood of this event occurring is high due to the thick, sulfuric clouds in the Venusian atmosphere. However, the intensity of this risk is lowly rated at a 2 due to the autonomous nature of the altitude control system. Of course, communications blackout will entail data backlogs; however, VISTA is assumed to be in safe altitude equilibrium during a blackout. We denote the communications technology with a TRL of 5, as it is successful on the ground but has yet to be tested in situ. Long Term Corrosion is assessed a likelihood rating of 5 and an intensity factor of 3. Unfortunately, long term corrosion is guaranteed to occur along the lifespan of VISTA. However, this corrosion effect is considered when developing the mission requirements. In the structure and materials section, we assess Teflon to be able to withstand the effects of corrosion for thirty days. Thus, this risk increases in likelihood in the extended mission. Given the track record of the structural materials used in previous missions, we award the structural technologies with a rating of 7.

## CDR Plan

### Long Lead Items

The first item of procurement that should be mentioned is the FLIR A700 STD Science Kit from TEquipment. This kit is equipped with Gigabit Ethernet and can handle the intense temperature range that VISTA will experience. Although this is a COTS component, it falls in the long lead section as there are several adjustments that need to be made to the product for functionality in VISTA. The expectation of the FLIR A700 is to handle any necessary imaging required from VISTA's scientific mission goals.



Figure 7: TEquipment FLIR A700 Science Kit [4]

A second long lead item is a custom pressure and temperature sensor suite capable of operating in the extreme conditions expected during the mission. Sensors rated for near-space or upper-atmospheric use often need to be specially ordered. A sensor of particular interest is the MET4-4A from Parascientific. In this case, the sensor must be modified to meet size, weight, and interface constraints, which can introduce additional delays. Given their importance in thermal modeling and environmental data collection, these sensors are crucial and should be addressed foremost in CDR.



Figure 8: MET4 and MET4-A from Parascientific [6]

Another key long lead component is the structural mounting assembly, including precision-machined brackets, fasteners, and thermal insulation elements. These mounts must be designed to securely hold scientific equipment like the FLIR camera while minimizing thermal gradients and vibration during ascent. As VISTA plans to have a corrosion resistant wrapping around the truss structure, this falls later into consideration for the design. Machining and integrating with materials such as multilayer insulation (MLI) or aerospace-grade foam can involve significant lead times, especially if modifications are needed after the first fabrication run. In regards to the location of this structure, please reference the initial concept devised in the SRR.

Finally, the mission will require a high-performance onboard computer or data acquisition unit (DAQ) to collect, store, and potentially pre-process science data. These systems face component shortages and long supplier lead times, particularly if custom firmware or breakout boards are needed for interfacing with sensors and cameras. Therefore, it had been identified as a long lead item and the modularity of such system should be heavily considered for CDR. These units also play a critical role in system integration and power budgeting, so they should be identified and ordered as early as possible to avoid downstream delays.



## References

- [1] Archimedes' principle - explanation and examples. <https://byjus.com/physics/archimedes-principle/>. Accessed: 2025-04-10.
- [2] Configured spectroradiometer systems. <https://internationallight.com/product-group/configured-spectroradiometer-systems>. Accessed: 2025-04-10.
- [3] Davinci mission overview. <https://science.nasa.gov/mission/davinci/>. Accessed: 2025-04-10.
- [4] Flir a700-std-science-kit scientific thermal imagers. <https://www.tequipment.net/FLIR/A700-STD-SCIENCE-KIT/Scientific-Thermal-Imagers/>. Accessed: 2025-04-10.
- [5] Interface region imaging spectrograph (iris). <https://iris.gsfc.nasa.gov/>. Accessed: 2025-04-10.
- [6] Model 80 met4-4a meteorological measurement system. [https://paroscientific.com/pdf/D80\\_MET4\\_4A.pdf](https://paroscientific.com/pdf/D80_MET4_4A.pdf). Accessed: 2025-04-10.
- [7] Satellite icons - flaticon. <https://www.flaticon.com/search?word=satellite>. Accessed: 2025-04-10.
- [8] Satellite ui design project. <https://www.figma.com/files/team/1491213761961480492/project/364000578>. Accessed: 2025-04-10.
- [9] Venus climate orbiter "akatsuki" (planet-c). [https://global.jaxa.jp/projects/sas/planet\\_c/](https://global.jaxa.jp/projects/sas/planet_c/). Accessed: 2025-04-10.
- [10] Venus fact sheet. <https://nssdc.gsfc.nasa.gov/planetary/factsheet/venusfact.html>. Accessed: 2025-05-06.
- [11] Veritas mission overview. <https://science.nasa.gov/mission/veritas/>. Accessed: 2025-04-10.
- [12] Dean McClements and Joel Schadeegg. All about polyether ether ketone (peek). <https://www.xometry.com/resources/materials/polyether-ether-ketone/>. Accessed: 2025-04-10.
- [13] Alvin Seiff, John T. Schofield, Arvydas J. Kliore, Fred W. Taylor, Sanjay S. Limaye, Henry E. Revercomb, Lawrence A. Sromovsky, Viktor V. Kerzhanovich, Vladimir I. Moroz, and Mikhail Ya. Marov. Models of the structure of the atmosphere of venus from the surface to 100 kilometers altitude. *Science*, 231(4744):1407–1408, 1986.
- [14] Yunchou Xing, Frank Hsieh, Amitava Ghosh, and Theodore S. Rappaport. High altitude platform stations (haps): Architecture and system performance. In *2021 IEEE 93rd Vehicular Technology Conference (VTC-Spring)*, pages 1–6, 2021.

# Appendices

## Appendix A: Balloon Code

```
1
2 %% Hot Air Balloon Volume Optimization
3
4 %Optimization
5
6 clear all
7 close all
8 clc
9
10 % Initializing the parameters for the optimization
11
12 Xi = [200, 1.2 , 350]; %Initial guess
13 A = [];
14 b = [];
15 Aeq = [];
16 beq = [];
17 lb = [0, 1 , 200];
18 ub = [1000, 2, 500];
19 phi = 1;% Limite angle for the circle approximation for the meridian
20
21 xSol = fmincon(@fObj,Xi, A,b,Aeq,beq,lb,ub, @Ceq);% Optimization. Must return
    optimal values for H, A and rc.
22
23
24 % We re-run the ODE45 with the optimized parameter to get the optimal solution
    for r
25
26 X0Opt = [xSol(3).*sind(phi); cotd(phi)]; %IC for ODE45
27 ZspanOpt = linspace(xSol(3)*(1-cosd(phi)),xSol(1) ,1000); %Span for z
28
29 options = odeset('RelTol',1e-7); % refine the discretization to get smooth
    curve for r
30 OptSol = ode45(@(z,x) [x(2); (1+x(2).^2).*(1-xSol(2)*(x(1)/xSol(1)).^0.5)./x(1)
    -2./(xSol(1)*xSol(3))*(1+x(2).^2).^(3/2)*(xSol(1)-z)*exp(2*xSol(2)*(x(1)/
    xSol(1)).^0.5)], ZspanOpt , X0Opt, options);
31
32 % for small values of z, we interpolate the meridian as a circular curve
33 % (see Irvine and Montauban)
34 %Here is the definition of the circle
35
36 PhiExtra = linspace(0.1,phi,10);
37 ZExtra = xSol(3)*(1-cosd(PhiExtra));
38
39 %We can compute the various parameters of interest for this extrapolation
40
41 Ro = xSol(3).*sind(PhiExtra);
42 Yo = cotd(PhiExtra);
43
44 %We can patch our extrapolation for small z data to our optimal solution to
    %get the full meridian
45
```

```

46
47 OptR = [Ro, OptSol.y(1,:)];
48 OptY = [Yo, OptSol.y(2,:)];
49 Zc = [ZExtra, OptSol.x];
50
51 % We can plot the meridian
52 figure
53 plot(OptR,(xSol(1)-Zc),'b')
54 axis equal
55
56 %And get the volume of the balloon generated
57
58 -fObj(xSol')
59
60
61 %%%%%%%%%%%%%%%%%%%%%%%%%%%%%%%%%%%%%%%%%%%%%%%%%%%%%%%%%%%%%%%%%%%%%%%%%
62
63 % Gore creation
64
65 S = zeros(1,length(OptR));
66
67 % we compute the arclength along the meridian for each z spanned.
68
69 for II=2:length(S)
70
71     S(1,II) = trapz(Zc(1,1:II), (1+(OptY(1,1:II)).^2).^(1/2));
72
73 end
74
75 % Gore envelope following the methode given in class
76
77 figure
78 plot(pi*OptR/12,270-S,'b')
79 hold on
80 plot(-pi*OptR/12,270-S,'b')
81 axis equal
82 set(gca,'visible','off')

```

```

1
2 function [c, ceq] = Ceq(X)
3
4 %Instanciating our vector of non linear equality constrain
5 ceq = zeros(3,1);
6
7 %Parameters definition
8
9 H = X(1);
10 A = X(2);
11 Rc = X(3);
12 phi = 1;
13
14 % Initializing parameters for ODE45
15
16 X0 = [Rc*sind(phi); cotd(phi)];
17 Zspan = linspace(Rc*(1-cosd(phi)),H ,1000);

```

```

18
19
20 Sol = ode45(@(z,x) [x(2); (1+x(2).^2).*(1-A*(x(1)/H).^0.5)./x(1)-2./(H*Rc)*(1+x
    (2).^2).^3/2*(H-z)*exp(2*A*(x(1)/H).^0.5)], Zspan , X0);
21
22 %Sol.x gives z
23 %Sol.y(1) gives r
24 %Sol.y(2) gives y
25
26 c = []; %We set the vector of unequality non linear constrain to zero since we
    don't have any
27 % Computing the components of our equality constrain vector
28
29 ceq(1,1) = trapz(Sol.x, (ones(1,length(Sol.y))+(Sol.y(2,:)).^2).^(1/2))-270;
30 ceq(2,1) = Sol.y(1,end)-30;
31 ceq(3,1) = Sol.y(2,end);
32
33
34 end

```

```

1
2 function [ V ] = fObj(X)
3
4 %Parameters definition
5 H = X(1);
6 A = X(2);
7 Rc = X(3);
8
9 % Initializing parameters for ODE45
10 phi = 1;
11 X0 = [Rc*sind(phi); cotd(phi)];
12 Zspan = linspace(Rc*(1-cosd(phi)),H ,1000);
13
14 Sol = ode45(@(z,x) [x(2); (1+x(2).^2).*(1-A*(x(1)/H).^0.5)./x(1)-2./(H*Rc)*(1+x
    (2).^2).^3/2*(H-z)*exp(2*A*(x(1)/H).^0.5)], Zspan , X0);
15 %Sol.x gives z
16 %Sol.y(1) gives r
17 %Sol.y(2) gives y
18
19 %Computation of -Volume, the thing we want to optimize
20
21 V = -pi*trapz(Sol.x , Sol.y(1,:).^2);
22
23
24 end

```

## Appendix B: Electric Propulsion Code

```

1
2 %% Script for 3 Low-Thrust Maneuvers (LEO --> LV0)
3 % Justin Bak -- 4/28/2025
4
5 clear

```

```

6 close all
7 clc
8
9 %% Parameters
10
11 % Hall Effect Thruster
12 T = 0.083; % assume constant thrust (N)
13 Isp = 1500; % 1000-8000 for HET (s)
14 mo = 200; % mass of structure, payload, etc. (kg)
15
16 %% Establish Constants
17
18 % Gravitational constants
19 G = 6.6743e-11;
20 g0 = 9.81;
21
22 % Masses
23 m_E = 5.972e24; % Mass of Earth (kg)
24 m_V = 4.870e24; % Mass of Venus (kg)
25 m_S = 1.988e30; % Mass of Sun (kg)
26
27 % mu of each body
28
29 mu_E = G*m_E;
30 mu_S = G*m_S;
31 mu_V = G*m_V;
32
33 % Establish structure variables
34
35 c.ue = Isp*g0;
36 ue = c.ue;
37 c.mdot = T/ue;
38
39 %% Establish Radii
40
41 %Earth
42 r_E = 6376*1000;
43 r_LEO = r_E + 600*1000;
44 r_ES = 149e9;%semimajor axis around sun
45 r_EE = r_ES*(m_E/m_S)^(2/5);
46
47 % Venus
48
49 r_V = 6051.8e3;
50 r_LV0 = r_V + 200e3;
51 r_VS = 108.2e6; %semimajor axis around sun (assuming circular
    orbits)
52 r_VE = r_VS*(m_V/m_S)^(2/5);
53
54 % Set final time
55
56 tf = 1e7;
57
58 %% BURN 1: r_LEO -> r_EE
59 disp("Initial Mass: " + mo + "kg")

```

```

60 % [t, vec] = odeCall(r0,rf,mu,tf,mo,c)
61 [t, vec] = odeCall(r_LEO,r_EE,mu_E,tf,mo,c);
62 dv1 = sqrt(mu_E/r_LEO)-sqrt(mu_E/r_EE);
63 ti = t(end);
64 mf = vec(end,5);
65 disp("Burn 1 Time: " + t(end)/3600/24 + "days")
66 disp("Burn 1 Final Mass: " + mf + "kg")
67
68 %% BURN 2: r_ES + r_EE -> r_VS - r_VE
69 % [t, vec] = odeCall(r0,rf,mu,tf,mo,c)
70 [t, vec] = odeCall(r_ES+r_EE,r_VS-r_VE,mu_S,tf,mf,c);
71 dv2 = sqrt(mu_S/(r_ES+r_EE))-sqrt(mu_S/(r_VS-r_VE));
72 ti = ti + t(end);
73 mf = vec(end,5);
74 disp("Burn 2 Time: " + t(end)/3600/24 + "days")
75 disp("Burn 2 Final Mass: " + mf + "kg")
76
77 %% BURN 3: r_VE -> r_LV0
78 r0 = r_LV0;
79 % [t, vec] = odeCall(r0,rf,mu,tf,mo,c)
80 [t, vec] = odeCall(r_LV0,r_VE,mu_V,tf,mf,c);
81 dv3 = sqrt(mu_V/r_LV0)-sqrt(mu_V/r_VE);
82 mf = vec(end,5);
83 ti = ti + t(end);
84 disp("Burn 3 Time: " + t(end)/3600/24 + "days")
85 disp("Burn 3 Final Mass: " + mf + "kg")
86 dv_total = dv1 + dv2 + dv3;
87 t_total = ti;
88 mp = mo-mf;
89 P = c.mdot*c.ue^2/2;
90 disp("Total Time: " + t_total/3600/24/365 + "years")
91 disp("Mp: " + mp + "kg")
92 disp("DeltaV total: " + dv_total/1000 + "km/s")
93 disp("Power Required: " + P/1000 + "kW")
94
95 %% Extract data from the ODE45 Solution
96 r = vec(:,1); %Hint: remember the order you put your initial conditions in
97 rdot = vec(:,2);
98 th = vec(:,3);
99 thdot = vec(:,4);
100 m = vec(:,5);
101
102 % Convert to Cartesian coordinates for plotting
103 x = r.*cos(th);
104 y = r.*sin(th);
105
106 %% Plot the Spiral Trajectory
107 figure
108 plot(x,y,'k--');
109 hold on
110 th = linspace(0,2*pi,1000);
111 r2 = r_VE;
112 xLEO = r0.*cos(th);
113 yLEO = r0.*sin(th);
114 xGEO = r2.*cos(th);

```

```

115 yGEO = r2.*sin(th);
116
117 plot(xLEO,yLEO,'b','LineWidth',2)
118 plot(xGEO,yGEO,'r--','LineWidth',2)
119
120 cost = mp;
121 function [t,vec] = odeCall(r0,rf,mu,tf,mo,c)
122     p.mu = mu;
123     tspan = [0,tf];
124     thetadot0 = sqrt(mu/r0^3);
125     S0 = [r0, 0, 0, thetadot0, mo]';
126
127     optS = @(t,S) opt1(t,S,rf);
128     options = odeset('Events', optS);
129
130     LTfun = @(t,S) odefun_skeleton(t,S,p,c);
131
132     [t,vec] = ode45(LTfun,tspan,S0,options);
133 end
134
135 function [value, isterminal, direction] = opt1(~,X,rf)
136 value = X(1) - rf;
137 isterminal = 1;
138 direction = 0;
139 end

```

```

1
2 function dS = odefun_skeleton(~, S, p, c)
3     % S = [r; rdot; theta; thetadot; m]
4     r      = S(1);
5     rdot   = S(2);
6     theta  = S(3);
7     thetadot = S(4);
8     m      = S(5);
9
10    mu = p.mu;
11
12    % Tangential thrust (low-thrust, spiral out)
13    T = c.mdot * c.ue;
14    a_tangential = T / m;
15
16    % Equations of motion
17    drdt      = rdot;
18    d2rdt2    = r*thetadot^2 - mu/r^2; % No thrust in radial direction
19    dthetadt  = thetadot;
20    d2thetadt2 = (a_tangential - 2*rdot*thetadot)/r;
21    dmdt      = -c.mdot;
22
23    dS = [drdt; d2rdt2; dthetadt; d2thetadt2; dmdt];
24 end

```

## Appendix C: Chemical Propulsion Code

```

1
2 % Clear variables, command window, and close all figures
3 clear all;
4 clc;
5 close all;
6
7 % Gravitational Constant
8 G = 6.67430e-11; % m^3/(kg s^2)
9
10 % Masses of celestial bodies
11 m_E = 5.972e24; % Mass of Earth (kg)
12 m_V = 4.870e24; % Mass of Venus (kg)
13 m_S = 1.988e30; % Mass of the Sun (kg)
14
15 % Gravitational parameters
16 mu_E = G * m_E; % Earth (m^3/s^2)
17 mu_S = G * m_S; % Sun (m^3/s^2)
18 mu_V = G * m_V; % Venus (m^3/s^2)
19
20 %% Part 1: LEO to Escape (Earth-Centered Hohmann Transfer)
21 % Constants for Earth-centered orbit
22 R_E = 6378 * 10^3; % Radius of Earth (m)
23 r_LEO = 6700 * 10^3; % Radius of LEO (m)
24
25 % Escape radius of Earth's sphere of influence
26 r_ES = 149e9; % Semi-major axis of Earth's orbit around the
    Sun (m)
27 r_esc = r_ES * (m_E / m_S)^(2/5); % Sphere of Influence (m)
28
29 % Hohmann transfer from LEO to escape
30 r_p = r_LEO; % Periapsis (LEO)
31 r_a = r_esc; % Apoapsis (escape)
32 a_transfer = (r_p + r_a) / 2; % Semi-major axis of transfer orbit
33
34 % Orbital velocities for Earth-centered transfer
35 v_LEO = sqrt(mu_E / r_LEO); % Initial velocity in
    LEO
36 v_transfer_p = sqrt(mu_E * (2 / r_p - 1 / a_transfer)); % Velocity at periapsis
37 delta_v1_LEO_to_escape = v_transfer_p - v_LEO; % Delta-v for LEO to
    escape
38
39 % Escape velocity at Earth's sphere of influence
40 v_esc_SOI = sqrt(mu_E / r_esc);
41
42 T_transfer_1 = pi * sqrt(a_transfer^3 / mu_E);
43
44 %% Part 2: Interplanetary Hohmann Transfer (Earth to Venus)
45 % Constants for Sun-centered orbit
46 AU = 1.496e11; % Astronomical Unit (m)
47 a_E = 1 * AU; % Semi-major axis of Earth's orbit (m)
48 a_V = 0.723 * AU; % Semi-major axis of Venus' orbit (m)
49
50 % Hohmann Transfer from Earth to Mars
51 r_p = a_E; % Periapsis (Earth's orbit)

```



```

52 r_a = a_V; % Apoapsis (Venus' orbit)
53 a_transfer = (r_p + r_a) / 2; % Semi-major axis of transfer orbit
54
55 % Orbital velocities in heliocentric orbits
56 v_E = sqrt(mu_S / r_p); % Earth's orbital velocity
57 v_V = sqrt(mu_S / r_a); % Venus' orbital velocity
58 v_transfer_p = sqrt(mu_S * (2 / r_p - 1 / a_transfer)); % Velocity at
    periapsis of transfer orbit
59 v_transfer_a = sqrt(mu_S * (2 / r_a - 1 / a_transfer)); % Velocity at apoapsis
    of transfer orbit
60
61 % Delta-v calculations for interplanetary transfer
62 delta_v2_departure = v_transfer_p - v_E; % Boost from Earth's orbit to transfer
    orbit
63 delta_v3_arrival = v_V - v_transfer_a; % Mars insertion delta-v
64
65 % Total interplanetary delta-v
66 delta_v_interplanetary = delta_v2_departure + delta_v3_arrival;
67
68 T_transfer_2 = pi * sqrt(a_transfer^3 / mu_S);
69
70 %% Part 3: Venus to enter LVO
71 % Constants for Venus-centered orbit
72 R_V = 6051.8 * 10^3; % Radius of Venus (m)
73 r_LMO = R_V + 200 * 10^3; % Radius of Low Venusian Orbit (LVO) (
    m)
74 r_VS = 108.2e6; % semimajor axis around mars sun (
    assuming circular orbits)
75 r_esc_V = r_VS*(m_V/m_S)^(2/5);
76 % Velocity at Venus SOI
77 v_V_SOI = sqrt(mu_V / r_esc); % Velocity at Mars SOI (m/s)
78
79 % Hohmann transfer from Venus SOI to LMO
80 r_p = r_LMO; % Periapsis (LMO)
81 r_a = r_esc_V; % Apoapsis (Venus SOI)
82 a_transfer_V = (r_p + r_a) / 2; % Semi-major axis of transfer orbit
83
84 % Orbital velocities for Mars-centered transfer
85 v_SOI_capture = sqrt(mu_V * (2 / r_a - 1 / a_transfer_V)); % Velocity at
    Mars SOI in transfer orbit
86 v_LMO = sqrt(mu_V / r_LMO); % Velocity in
    LMO
87 v_transfer_p_Venus = sqrt(mu_V * (2 / r_p - 1 / a_transfer_V)); % Velocity at
    periapsis
88
89 delta_v4_SOI_to_LVO = v_transfer_p_Venus - v_LMO; % Delta-v for SOI to LMO
90
91 T_transfer_3 = pi * sqrt(a_transfer_V^3 / mu_V);
92 %% Total Delta-v
93 % Total delta-v including LEO escape, interplanetary transfer, and Mars capture
94 delta_v_tot = delta_v1_LEO_to_escape + delta_v_interplanetary +
    delta_v4_SOI_to_LVO;
95 T_transfer_total = T_transfer_1 + T_transfer_2 + T_transfer_3;
96 % Display results
97 fprintf('Delta-v for LEO to escape: %.2f m/s\n', abs(delta_v1_LEO_to_escape));

```

```

98 fprintf('Delta-v for interplanetary departure: %.2f m/s\n', abs(
    delta_v2_departure));
99 fprintf('Delta-v for Venus arrival: %.2f m/s\n', abs(delta_v3_arrival));
100 fprintf('Delta-v for Venus SOI to LV0: %.2f m/s\n', abs(delta_v4_SOI_to_LV0));
101 fprintf('Total Delta-v: %.2f m/s\n', abs(delta_v_tot));
102 fprintf('Transfer time for Venus SOI to LV0: %.2f seconds (%.2f days)\n',
    T_transfer_total, T_transfer_total/ (24 * 3600));

```